

STABILITY STUDY OF THE HIGHER ORDER MODE BEAM POSITION MONITORS AT THE ACCELERATING CAVITIES AT FLASH*

L. Shi ^{a,b,#}, N. Baboi ^a, R.M.Jones ^b

^a DESY, Hamburg, Germany, ^b The University of Manchester, UK

Abstract

When electron beams traverse an accelerating structure, higher order modes (HOMs) are excited. They can be used for beam diagnostic purposes. Both 1.3 GHz and 3.9 GHz superconducting accelerating cavities at FLASH linac, DESY, are equipped with electronics for beam position monitoring, which are based on HOM signals from special couplers. These monitors provide the beam position without additional vacuum components and at low cost. Moreover, they can be used to align the beam in the cavities to reduce the HOM effects on the beam. However, the HOMBPM (Higher Order Mode based Beam Position Monitor) shows an instability problem over time. In this paper, we will present the status of studies on this issue. Several methods are utilized to calibrate the HOMBPMs. These methods include DLR (Direct Linear Regression), and SVD (Singular Value Decomposition). We found that SVD generally is more suitable for HOMBPM calibration. We focus on the HOMBPMs at 1.3 GHz cavities. Techniques developed here are applicable to 3.9 GHz modules. The work will pave the way for HOMBPMs of the E-XFEL (European X-ray Free Electron Laser).

INTRODUCTION

FLASH (Free-electron-LASer in Hamburg) [1] is a FEL (Free Electron Laser) facility to generate XUV (Extreme Ultraviolet radiation) and soft X-ray by the so-called SASE (Self Amplified Spontaneous Emission) process from energetic electron beam bunches. The beam is accelerated by seven 1.3 GHz modules that each of them has eight TESLA cavities working at 1.3 GHz and one 3.9 GHz module with four 3.9 GHz cavities. Each cavity has two HOM (Higher Order Mode) couplers to minimise the effects from the beam excited HOMs. The HOMs are brought out of the module to room temperature via cables.

There are in total 78 channels of HOM signal. All channels are equipped with independent down converter electronics. For the 1.3 GHz modules, electronics are designed by SLAC. The electronics designed by Fermilab for the 3.9 GHz module are being commissioned.

HOMBPMs have been demonstrated good performance [2, 5]. They have a great potential to reduce the number of conventional BPMs which are relative expensive along the linac. This is especially desirable for facilities which have long linac such as ILC [3] etc.

However, we found in the past that the HOMBPM systems at FLASH are not stable. They perform good after immediate calibration but the results become inconsistent after some time, from several hours to days.

In this paper, we first briefly present the basic principle of a HOMBPM and procedures for its calibration. Then we move to the methods we used to calibrate them. The results are shown in the last section. Future work and final remarks conclude the paper.

PRINCIPLE OF HOMBPM

When an electron beam traverses a cavity, HOMs are excited. We can classify them by the azimuthal dependence into ‘Monopole’, ‘Dipole’ etc. [4].

Among these modes, dipole modes have linear dependence on the beam offset relative to the electrical centre of the cavity [5].

A dipole mode at around 1.7 GHz has been selected for such purpose in the TESLA cavity since it has strong coupling to the beam. Thus it provides high sensitivity to the beam position offset [5].

Figure 1 shows a block diagram of a HOMBPM system.

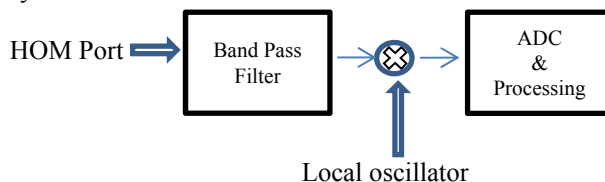


Figure 1: Block diagram of HOMBPM system.

The HOM signal is band filtered at around 1.7 GHz and down mixed with a signal from local oscillator. The signal is sampled and further transmitted to DOOCS (Distributed Object Oriented Control System) [6]. A user defined program was developed to perform data acquisition and post processing.

DATA DESCRIPTION AND MODEL OVERVIEW

Based on the HOMBPM system described above, the HOM data were gathered over half a year and are still under monitoring. The data was taken normally when FLASH operated in single bunch mode. The bunch repetition rate is 10 Hz. Most datasets were taken parasitically and we have four datasets that we moved the beam in a wide range. The data includes bunch charge from toroid readouts, the beam position from two cavity BPMs located upstream and downstream of the accelerating module and HOM signals from both HOM

*The work is part of EuCARD², partly funded by the European Commission, GA 312453
[#] liangliang.shi@desy.de

couplers. This paper is based on data from accelerating module 5.

The main reason for the resolution drift of a HOMBPM is that it needs to ‘remember’ the complete information of past beam positions in order to interpret a new beam position inside a cavity.

HOMBPM needs to be calibrated in order to make it be able to predict the beam position inside the cavity. When directly using the amplitudes of a dipole signal, one loses the phase information. Therefore, the whole waveform is used. Due to the linear dependence between the dipole signal and the beam offset, linear regression was performed to correlate the measured dipole waveform and the beam position from BPMs used for calibration.

The data is arranged in a matrix form as shown in equation 1.

$$\begin{bmatrix} d_{11} & \cdots & d_{1n} \\ \vdots & \ddots & \vdots \\ d_{m1} & \cdots & d_{mn} \end{bmatrix} \begin{bmatrix} C_{11} & C_{12} \\ \vdots & \vdots \\ C_{n1} & C_{n2} \end{bmatrix} = \begin{bmatrix} X_{11} & Y_{11} \\ \vdots & \vdots \\ X_{m1} & Y_{m1} \end{bmatrix} \quad (1)$$

Each row in the data matrix (d_{ij}) corresponds to one dipole waveform and the number of rows is the number of measurements available in a dataset. An additional column was placed in the data matrix to capture the intercept in the linear regression model.

The position matrix (X Y) was obtained by interpolating the beam position inside the cavity from the two BPMs. The calibration matrix C_{ij} obtained by linear regression is the knowledge of beam positions that calibration process can build into the HOMBPM.

Based on what it will actually be put in the data matrix, the model can be classified into DLR and SVD.

Each dataset is partitioned into two parts: one for calibration of the HOMBPM; the other independent part is used for validating its performance.

In this paper, the process of obtaining the calibration matrix is called training since we repeated the process several times from data mining point of view. The application of the calibration matrix to the validation dataset is called validation.

CALIBRATION PROCEDURE AND METHODS

An example of dipole signal from HOM coupler 2 of cavity 1 module 5 is shown in Fig. 2.

The signals from HOM ports are mixed with a so-called calibration signal from electronics which has nothing to do with the beam position [5].

Due to the trigger delay, there is a certain part (around 1 μ s) of signal at the beginning of a measured dipole waveform dominated by the calibration signal from the electronics.

The calibration signal was removed from the dipole signal by fitting the sinusoid waveform. The filtered dipole signal was further pre-processed to remove the transient part and a time window of fixed width was applied to the waveform to select the part of dipole for

regression. The motivation is mainly to avoid over training.

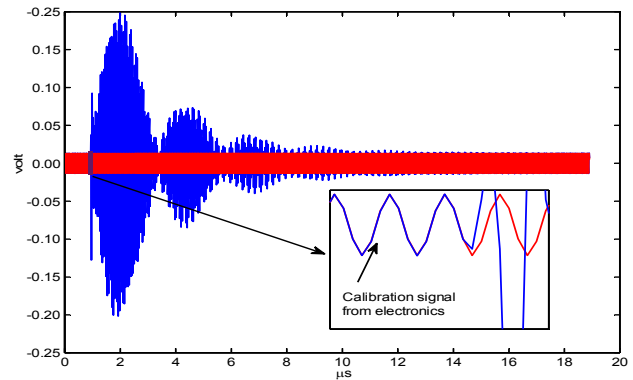


Figure 2: Dipole signal from HOM coupler 2 of 1st cavity at module 5. The calibration signal is highlighted with red colour and has a pure sinusoidal waveform.

In the DLR method, the pre-processed dipole signals are directly put in the data matrix. We can also transform the dipole signals and put them in the data matrix. In this paper, the transformed dipole mainly refers to the representation of a dipole signal by eigenmodes. The eigenmodes can be obtained via SVD (Singular Value Decomposition).

DLR

In the DLR method, we put the pre-processed dipole signal in the rows of a data matrix as shown in equation 2.

$$\begin{bmatrix} Dipole_{11} & 1 \\ \vdots & \vdots \\ Dipole_{m1} & 1 \end{bmatrix} \begin{bmatrix} C_{11} & C_{12} \\ \vdots & \vdots \\ C_{n1} & C_{n2} \end{bmatrix} = \begin{bmatrix} X_{11} & Y_{12} \\ \vdots & \vdots \\ X_{m1} & Y_{m2} \end{bmatrix} \quad (2)$$

In our analysis, the number of columns is fixed to 301 and the number of measurements (rows) varies from a few hundred to a few thousand, depending on the datasets.

The data was partitioned into training and validation parts based on ten folds cross validation. 90% of the data is used for training purpose and the other 10% of the data was used for validation. We repeated the training process 10 times to potentially use all the datasets for validation so that the model obtained is unbiased.

The resolution of HOMBPM for one dataset is defined as the RMS (Root Mean Square) of the difference between the position predicted from the model and the position interpolated from two BPMs.

Because we partitioned the dataset ten times, the average of the ten RMS values was treated as the resolution we can obtain for the HOMBPM from the dataset. The standard deviation of these ten RMS values was regarded as the model fluctuation. In Fig. 3 and Fig. 4, we show the obtained results for the training and validation datasets respectively. The result is based on the signals from HOM coupler 2 of the 1st cavity in module 5.

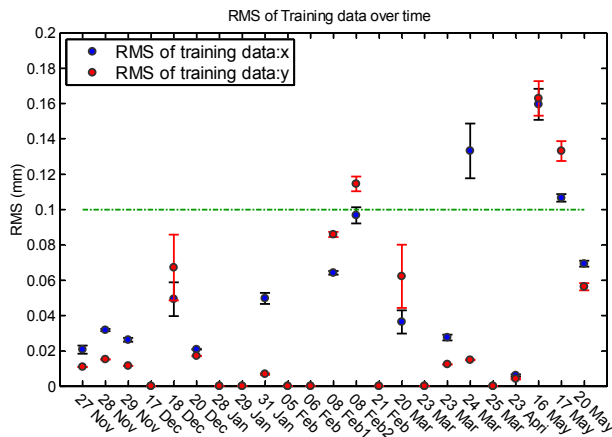


Figure 3: Resolution distributions of training datasets.

We can observe that several datasets were over trained (eg. 17 Dec, 28 Jan, and 29 Jan) because the number of measurements available is less than number of regressors in the DLR model. In such case, the model generally also loses the power of prediction which can be observed in the wide fluctuation of the resolution for the validation datasets in Fig. 4.

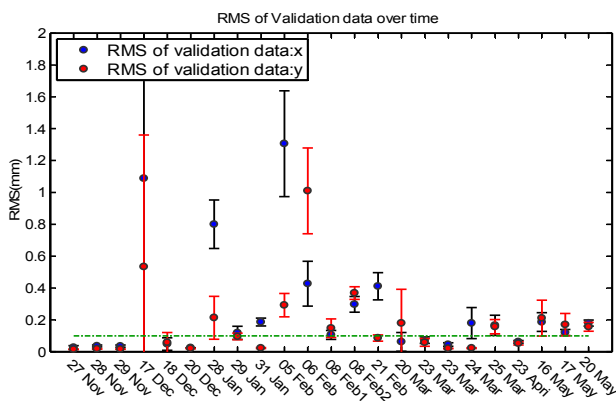


Figure 4: Resolution distributions of validation datasets.

Based on the Fig. 3 and Fig. 4, we can observe that some datasets can be better described by the DLR model (better resolution), but others show relatively worse resolution even if we exclude the results due to over training. The resolution of the HOMBPM spreads over hundreds of μm . We put a $100 \mu\text{m}$ green line in both plots. This is our first target to achieve. Even better resolution ($\sim 10 \mu\text{m}$) has been demonstrated in the past [2]. Due to the instability problem, the resolution can easily drift to hundreds of μm .

The model is simple to implement, but the drawback is that it needs more measurements to avoid over training. Due to the parasitic nature of the study, this is sometimes not possible. To better exploit the datasets obtained, the technique of multivariate data reduction was used. We tried several data mining techniques, but found that SVD method is more suitable for the task due to the intrinsic relation to the physical modes as we will discuss below.

SVD

SVD (Singular Value Decomposition) or principal component analysis are widely used for MIA (Model Independent Analysis) in computer science and physics. They are closely connected and mathematically equivalent.

From physics point of view, each dipole signal has two polarizations with the same resonant frequency if the cavity is cylindrically symmetric. In reality, these two polarizations are degenerated due to the broken symmetry by the couplers (power and HOM) and imperfections of the cavity.

In Fig. 5, we show the spectrum of a typical dipole signal based on 2048 points FFT (Fast Fourier Transform).

The frequency was reconstructed based on the sampling frequency of 108.3 MHz. We can observe the frequency gap between the two polarizations.

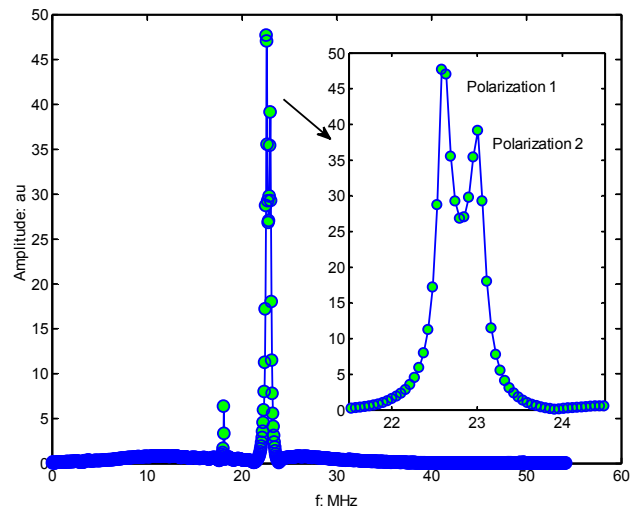


Figure 5: FFT of dipole waveform from Fig. 2. The sampling frequency is 108.3 MHz.

These two polarizations have linear dependence on the beam offset. One example is shown in Fig. 6.

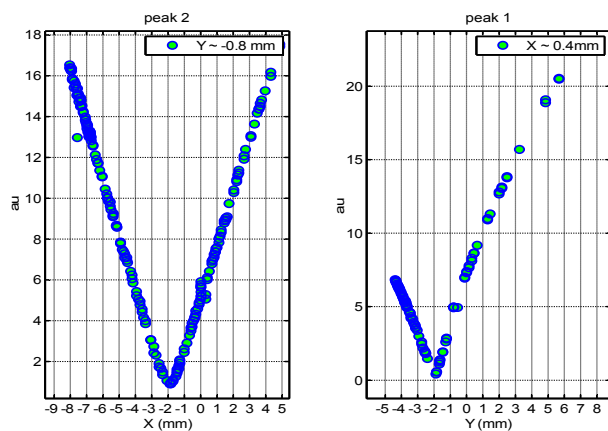


Figure 6: Position dependence of two polarizations (1) Y is about -0.8 mm; (2) X is about 0.4 mm.

Details of SVD discussion for HOMBPM calibration can be found in [5]. Normally the modes discovered by SVD or MIA are modes in the vector space. There is a great difficulty to correlate these modes in vector space with the HOMs that have physical meaning. However, there is a correspondence between the two polarizations (when they are excited) and the first two modes discovered by SVD method. These modes are referred as Eigen-dipoles in this paper. Eigen-dipole is a general term to describe the modes discovered by SVD method used in our calibration. Fig. 7 shows that the physical dipole spectrum and the first two modes discovered by SVD method. The spectrum was obtained by 2048 points FFT of a dipole waveform.

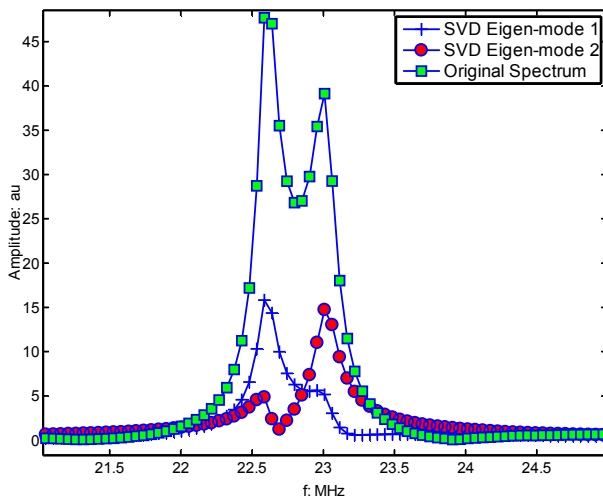


Figure 7: The identification of SVD modes and two polarizations of a dipole signal.

Amplitudes of these dipoles can be calculated via projecting the dipole waveforms onto Eigen-dipoles [2]. The amplitudes were arranged in the data matrix.

$$\begin{bmatrix} Amplitudes_{11} \\ \vdots \\ Amplitudes_{m1} \end{bmatrix} \begin{bmatrix} 1 \\ \vdots \\ 1 \end{bmatrix} \begin{bmatrix} C_{11} & C_{12} \\ \vdots & \vdots \\ C_{n1} & C_{n2} \end{bmatrix} = \begin{bmatrix} X_{11} & Y_{12} \\ \vdots & \vdots \\ X_{m1} & Y_{m2} \end{bmatrix} \quad (2)$$

Amplitudes in equation 2 refer to the amplitudes obtained in the space spanned by these Eigen-dipoles. The number of columns depends on the number of Eigen-dipoles used for the calibration. In our case, the number is fixed at 10 because we found 10 Eigen-dipoles are enough for calibration. So the number of columns in the data matrix is 11 in equation 2.

The results based on SVD method are displayed in Fig. 8 and Fig. 9 respectively.

Based on the SVD method, basically we removed the issue of over training. When the X position cannot be trained well (larger resolution than Y position), it also cannot predict well in X position (validation), and vice versa.

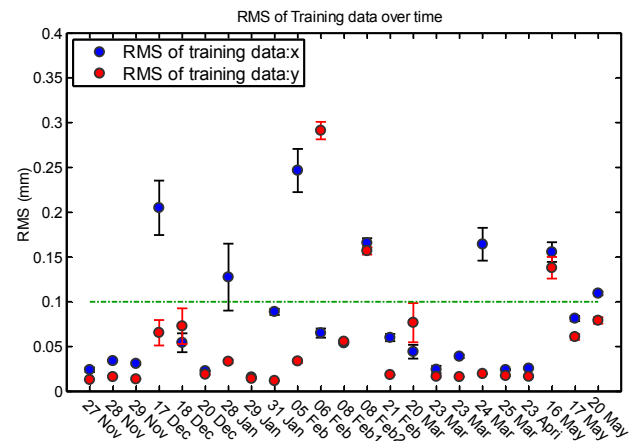


Figure 8: RMS distributions of training datasets over time based on SVD method. Top 10 Eigen-dipoles were used.

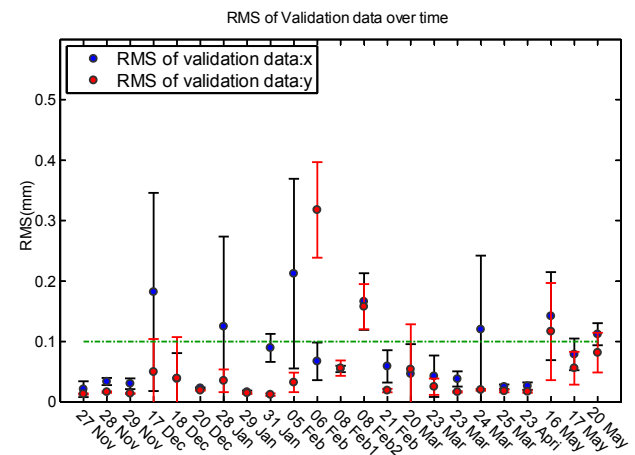


Figure 9: RMS distributions of validation datasets based on SVD method. Top 10 Eigen-dipoles were used.

From the error bar we observe that some datasets are sensitive (larger error bar) to the data partition, while others are not that sensitive.

We also can observe that the resolution varies hundreds of μm as we found with DLR method.

RESULTS SUMMARY OF DLR, SVD

The HOMBPM based on either DLR or SVD methods shows a spread of resolution over time. A summary of the calibration results based on DLR and SVD for is shown in Fig. 10.

After excluding the over trained results, both methods show resolution below 200 μm for most datasets. The resolution for calibration datasets varies a few hundred micro meters in both methods. For some datasets, we get hundreds of μm resolution in training datasets. Thus the resolutions obtained for the validation datasets are low or fluctuate widely.

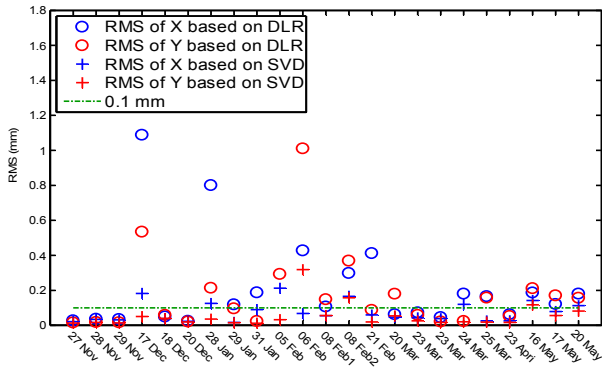


Figure 10: DLR and SVD summary. Only the mean values are displayed. The over trained results are also displayed in the plot.

In general, the SVD method performs better. When the resolution of the HOMBPM in X is worse than in Y in one method, it is also true in other method. That means both methods captured the essential information from the HOM data. However, there are two datasets (16 May, 17 May) showing inconsistency with this. We have not found out the reason yet.

Since the beam position is a strong factor in the formation of dipole signals, we plot the interpolated beam position over dates in Fig. 11.

The resolution of the HOMBPM varies a lot on some datasets. These datasets correspond to the case when the beam moves in a wider range and the beam position patterns show large gaps. One explanation would be that in such cases the HOMBPM cannot interpolate or extrapolate the position over the gap well.

One obvious drawback of such calibration scheme is that the HOMBPM is sensitive to the cavity BPMs used and their technical problems.

CONCLUSION AND OUTLOOK

We observed that the resolution changes (hundreds of μm) over time based on the same methods. We also saw a discrepancy between the two methods used, DLR and SVD, on the same datasets. Generally SVD performs better than DLR due to its intimate relationship to physical HOMs. We plan to use the SVD method to pre-select dipole waveforms before they can be used for calibration. We need to minimise the influence from the cavity BPMs.

Some unusual results are not completely understood yet.

Future work will focus on the stability of the dipole spectrum study. Data acquisition and analysis will continue for the 1.3 GHz modules. Recently we are commissioning the electronics of HOMBPM for 3.9 GHz module [7].

ACKNOWLEDGMENT

We thank FLASH team for the great supports for the work.

REFERENCES

- [1] <http://flash.desy.de/>
- [2] S.Molloy, "High precision superconducting cavity diagnostics with higher order mode measurements" PRST-AB 9, 112802 (2006).
- [3] <https://www.linearcollider.org/>
- [4] R.Wanzenberg, TESLA 2001-33, 2001.
- [5] J.Frisch, "Electronics and algorithms for HOM based beam diagnostics", AIP Conf.Proc. 868 (2006) 313-324.
- [6] <http://tesla.desy.de/docs/docs.html>
- [7] N.Baboi et al., "Commissioning of the Electronics for HOM-based Beam Diagnostics at the 3.9 GHz Accelerating Module at FLASH", IBIC2014, Monterey, TUPF10 (2014).

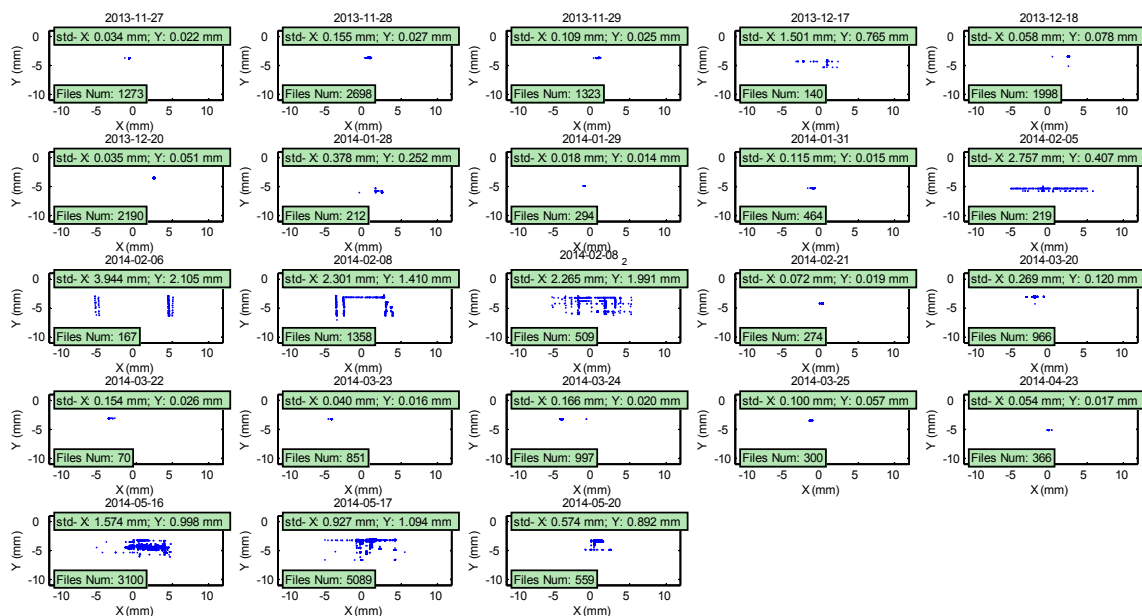


Figure 11: Interpolated beam position pattern over dates.